

PREDICTION OF STRATOSPHERIC OZONE CHANGE DUE TO NITROGEN OXIDES IN EXHAUST OF SUPERSONIC AIRPLANE

Hirotohi Kubota*, Tomonori Ushiyama, Tadaharu Watanuki***

***Department of Aeronautics and Astronautics, University of Tokyo, Tokyo 113-8656, Japan**

****Presently, Hitachi Company, Ltd.**

E-mail : k_16104@j02.itscom.net

Keywords: *Supersonic airplane, NO_x emission, Ozone-NO_x chemical reaction, Stratospheric ozone change*

Abstract

Experimental study on chemical reaction of ozone (O₃) and nitrogen oxides (NO_x) in a space chamber and numerical simulation of influence of NO_x emission from aircraft on stratospheric ozone change with the use of those chemical reactions are executed for the purpose of solution of one of the environmental issues for realization of next-generation Supersonic Transport (SST). The Fourier Transform Infrared Spectrometer (FT-IR) can be used as measurement technique for the necessary species concentration and the measured characteristics of chemical reaction of ozone and nitrogen oxides are discussed in comparison with analytical approach. The ozone change rate in the stratospheric atmosphere is estimated and total ozone rather increases by NO_x exhaust at altitude of 20 km, whereas the possibility of ozone depletion is not denied around altitude of 30 km and over.

1 Introduction

A forecast of air traffic demand by JADC (Japan Aircraft Development Corporation) suggests that the annual increase rate of RPK (Revenue Passenger Kilometer) in the world is 5.2 % during the years from 1984 to 2003 and 5.0 % from 2004 to 2023 [1]. The world RPK in 2023 will be 8.172 trillion which is approximately 2.64 times of the 2003's. Especially RPK in the area of Asia-Pacific is

higher than average of the world. In order to satisfy these future passenger demands, both the performance of high-speed and large amount of air transport is needed.

A supersonic airplane is effective and important from the standpoint of high-speed transportation. Although the "Concorde" which was a sole commercial supersonic airplane has been retired, the next-generation supersonic transport (SST) should be realized by overcoming the critical issues of technologies accomplishment, market viability and environmental compatibility [2].

One of the environmental issues for the next-generation supersonic transport is the effect of exhausted gas on stratospheric ozone layer. Among the various species included in the emitted gas from airplane engine, nitrogen oxides (NO_x) are considered to be those that play major roles in destroying the ozone (O₃). Therefore, the both efforts of prediction and assessment of ozone chemistry with nitrogen oxides and improvement of combustor of airplane propulsion system for lower amount of nitrogen oxides are necessary [3], [4].

The present paper focuses on understanding of the chemical reactions of ozone (O₃) and nitrogen oxides (NO_x) and their simulation. The following two attempts are presented:

- (1) Experimental study on the chemical reactions in a space chamber, and
- (2) Numerical simulation of chemical reactions in the stratosphere with the flight scenario of SST and prediction of ozone change.

2 Experiment of Chemical Reactions of Ozone and Nitrogen Oxides in a Space Chamber

2.1 Experimental Method and Apparatus

The experimental apparatus consists of space chamber which simulates the environment of upper atmosphere, ozone generator, species concentration analyser, and FT-IR (Fourier Transform Infra-Red Spectrometer) as shown in Fig. 1 [3], [4].

Nitrogen Oxides are injected into the space chamber which is filled with the ozone of definitely determined amount in advance. The measured species concentrations by FT-IR are processed with use of PC (Personal Computer).

The details of each experimental apparatus are described below.

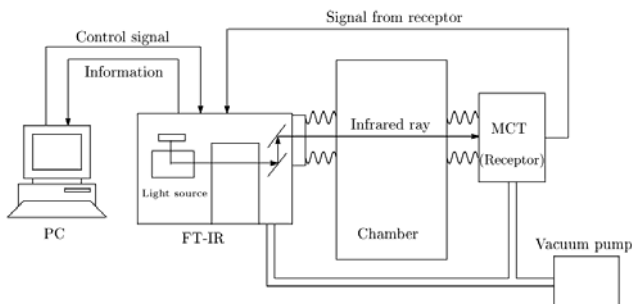


Fig. 1 Experimental Setup

2.1.1 Space Chamber

The experiment was conducted with the use of a space chamber in the Department of Aeronautics and Astronautics, the University of Tokyo as shown in Fig. 2, whose diameter and length are 2 meters and 3 meters, respectively. It has several flanges on its sides, front door, top, and bottom for measurement and observation. The inner pressure can be attained to less than 1.33×10^{-3} Pa by operating two rotary pumps, a high capacity mechanical booster pump, and an oil diffusion pump as its exhaust system.



Fig. 2 Space Chamber

2.1.2 Fourier Transformation Infrared Spectrometer

A Fourier Transform Infra-Red Spectrometer (FT-IR) [5] was used to measure the concentrations of gases. The device applies the Fourier transform infrared spectroscopy method, where the transmittance data of the wave number is obtained by Fourier transforming the interferogram. This interferogram is obtained from measurement of ceramic generated infrared light, which goes through an interferometer and then the sample. This optical measurement enables to measure gas concentration quickly and exert little influence on the sample gas. Water and carbon dioxide in the air interrupt measurement because they have a strong and wide absorption band in the infrared region, therefore a pump is used to create a vacuum inside the FT-IR and MCT receptor. The diagram of the interferometer is shown in Fig. 3.

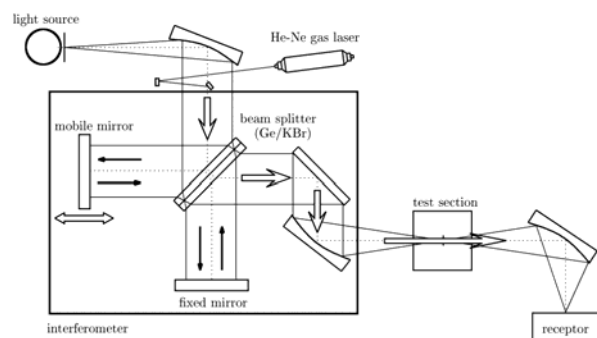


Fig. 3 Diagram of Interferogram

2.1.3 Ozone Generator and Automatic Ozone Analyzer

An ozone generator which has a capacity of generation up to 150 ppm and the flow rate of about 1~5 liters per minute was used to supply ozone to the chamber. In this device, oxygen molecules are dissociated to oxygen atoms when ultraviolet light is transmitted through air, and ozone is formed by combination of atomic and molecular oxygen.

An automatic ozone analyzer measures concentration of ozone by taking advantage of the property that ozone absorbs ultraviolet light of wavelength of 254 nm. Its response time is 20 seconds, and detectability is 0.02 ppm. This device was used for calibration of FT-IR measurement.

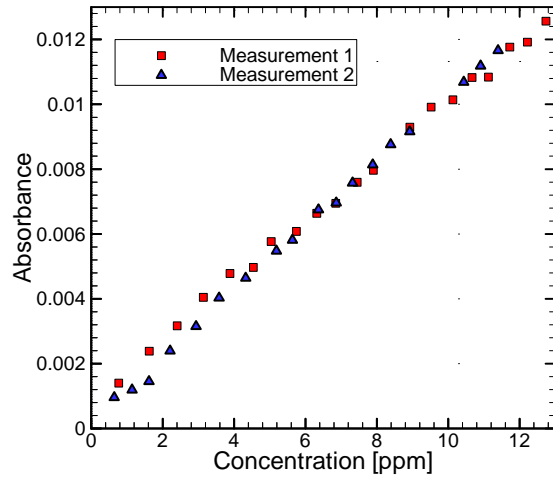


Fig. 4 O₃ Calibration

2.2 Experimental Results and Discussion

2.2.1 Calibration

Prior to the measurement of the species concentration, the calibration data of ozone, nitrogen monoxide, and nitrogen dioxide are obtained under the pressure of 5.5×10^3 Pa, which is approximately equal to the atmospheric condition at an expected SST flight altitude of 20 km.

The relationship between the concentration of ozone (O₃) and the absorbance (absorbance) measured by FT-IR at the wave number of $1,054.9 \text{ cm}^{-1}$ is shown in Fig. 4. The absorbance is almost linearly proportional to the concentration of ozone which is reasonable according to the Lambert-Beer's law. The repeatability of measurements 1 and 2 was also affirmed. The relationship between the concentration of ozone C and the absorbance A is shown in the equation below.

$$C_{O_3} = 9.747 \times 10^2 A_{O_3} \quad (1)$$

The relationships between the concentration and the absorbance for nitrogen monoxide (NO) and nitrogen dioxide (NO₂) at the wave number of $1,903.4 \text{ cm}^{-1}$ and $1,628.6 \text{ cm}^{-1}$, respectively, are shown in Fig. 5, which

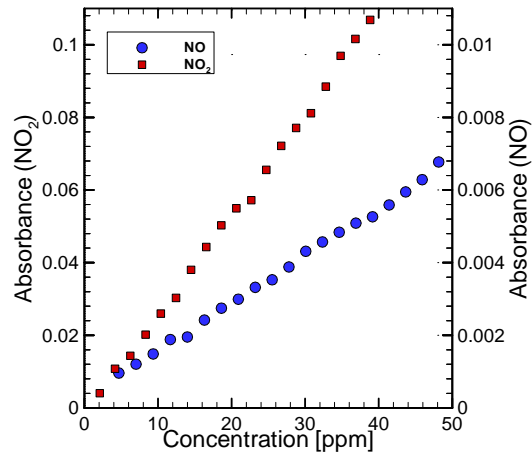


Fig. 5 NO and NO₂ Calibration

show the proportionality of the absorbance with the concentration as similar as the case of ozone. The relationship between the concentration C of nitrogen monoxide and nitrogen dioxide and the absorbance A is shown in the equation below.

$$C_{NO_3} = 7.19 \times 10^3 A_{NO} \quad (2)$$

$$C_{NO_2} = 3.71 \times 10^2 A_{NO_2} \quad (3)$$

Since the reduction of the concentration of ozone in the case where ozone alone was put in the chamber is very little, it is verified that the following experiments are caused only by the chemical reactions being investigated [3], [4].

2.2.2 O₃-NO_x Chemical Reactions

The time histories of the ozone concentration in the case of the reaction of O₃ - NO and the reaction of O₃ - NO₂ are shown in Figs.6 and 7 respectively. The NO₂ concentration of the above two cases are also shown in Figs.8 and 9 respectively.

As described later, dinitrogen pentoxide (N₂O₅) is generated in the chain of chemical reactions of ozone and nitrogen oxides, therefore the existence of dinitrogen pentoxide has important meanings in ozone chemistry. In Fig. 10 and 11, only the measured absorbance of dinitrogen pentoxide is shown because the calibration could not be done due to lack of its standard gas.

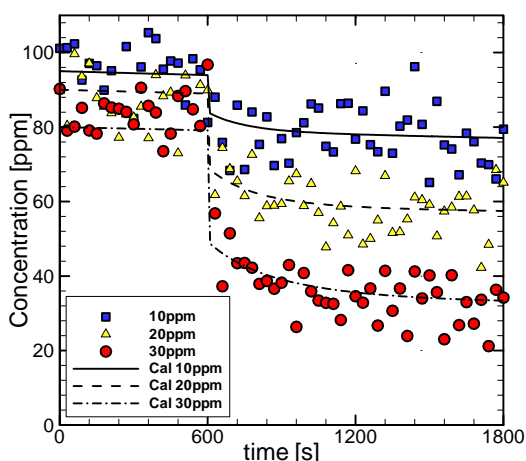


Fig. 6 Time History of O₃ Concentration at O₃-NO Reaction with Variation of Amount of NO Injection

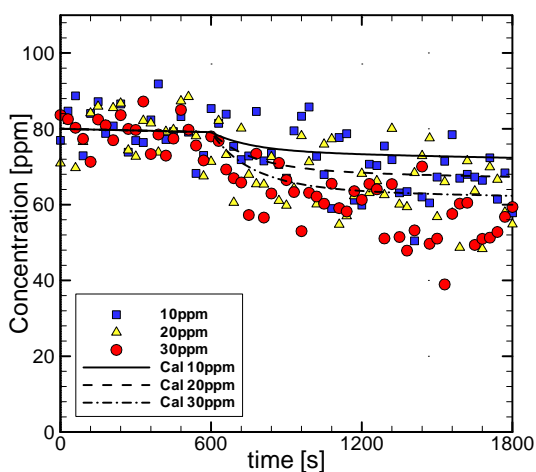


Fig.7 Time History of O₃ Concentration at O₃-NO₂ Reaction with Variation of Amount of NO₂ Injection

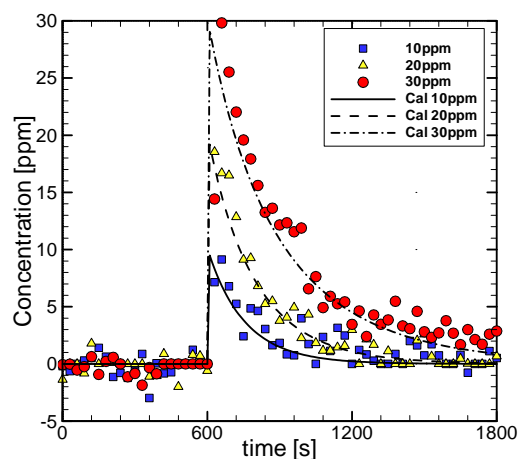


Fig. 8 Time History of NO₂ Concentration at O₃-NO Reaction with Variation of Amount of NO Injection

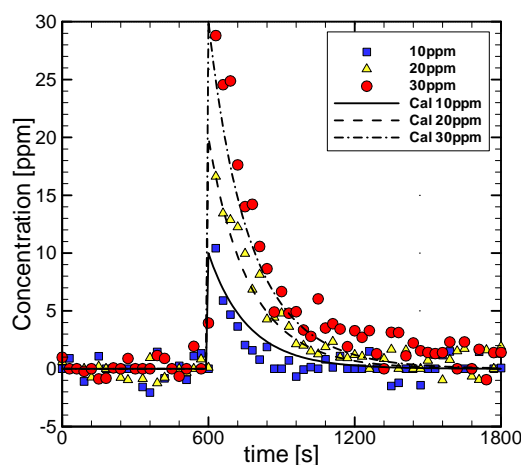


Fig. 9 Time History of NO₂ Concentration at O₃-NO₂ Reaction with Variation of Amount of NO₂ Injection

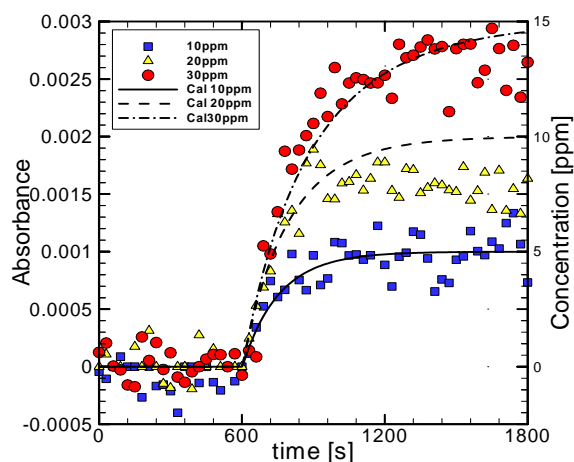


Fig. 10 Time History of N₂O₅ Concentration at O₃-NO Reaction with Variation of Amount of NO Injection

**PREDICTION OF STRATOSPHERIC OZONE CHANGE DUE TO NITROGEN OXIDES
IN EXHAUST OF SUPERSONIC AIRPLANE**

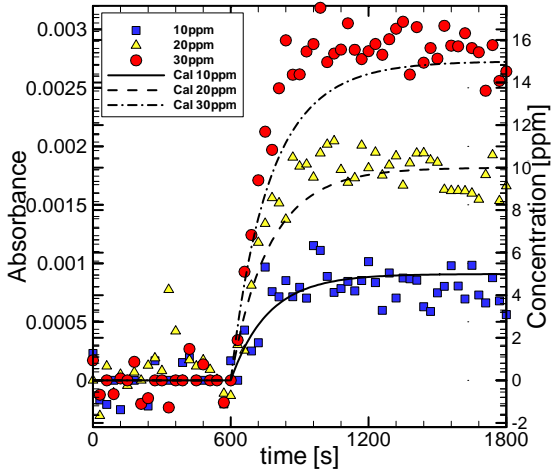


Fig. 11 Time History of N_2O_5 Concentration at O_3 - NO_2 Reaction with Variation of Amount of NO_2 Injection

Calculations of the associated chemical reactions were performed in order to verify the experimental data. In these calculations, parameters such as pressure, temperature, initial concentration of ozone, amount of NO_x injected, and time of injection were set equal to those of the experiments. Chemical reactions and rate constants used in the calculations are shown below as a function of temperature T .



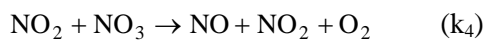
$$k_1 = 1.8 \times 10^{-12} \exp(-1370/T)$$



$$k_2 = 1.3 \times 10^{-11} \exp(250/T)$$



$$k_3 = 1.2 \times 10^{-13} \exp(-2450/T)$$



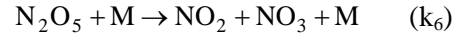
$$k_4 = 2.3 \times 10^{-13} \exp(-1000/T)$$



$$k_5 = \frac{k_0(T)[M]}{1 + k_\infty(T)[M]/k_0(T)} \times 0.6 \left\{ 1 + \left[\log_{10} \left(k_0(T)[M]/k_\infty(T) \right) \right]^2 \right\}^{-1}$$

$$\text{where, } k_0(T) = 2.2 \times 10^{-30} (T/300)^{-4.3},$$

$$k_\infty(T) = 1.5 \times 10^{-12} (T/300)^{-0.5}$$



$$k_6 = 6.0 \times 10^{14} \exp(-10970/T) / D$$

$$D = 7.0 \times 10^{21} \exp(-2670/T) + [M]$$

The results of the calculations are shown in Figs.6 to 11 along with the results of the experiments.

The findings from the experiment and calculation are as follows.

(1) The case of reactions between ozone and nitrogen monoxide (O_3 - NO reaction)

Since the calibration is conducted at 1.0×10^5 Pa in the ozone case, the data are scattered because noise is amplified at low pressures such as 5.5×10^3 Pa.

The concentration of ozone is reduced almost instantly at first by nearly the same amount as that of the injected nitrogen monoxide, and it continues to decrease gradually after the injection is completed (See Fig. 6). The total amount is approximately double that of the injected nitrogen monoxide. The concentration of nitrogen dioxide is zero until nitrogen monoxide is injected, and then increases instantly by nearly the same amount as that of the injected nitrogen monoxide (Fig. 8). After the initial increase, nitrogen dioxide is reduced quickly to a specific constant concentration.

As seen in Fig. 10, the absorbance of dinitrogen pentoxide starts to increase when nitrogen monoxide is injected, and converges to a certain constant concentration. These tendencies are observed in every case, and the results of the experiment give good agreement with the values obtained by the calculations, where the calculated concentration and experimentally obtained absorbance is correlated analytically.

The above results demonstrate the two-staged reactions, that is, the primary reaction

between ozone and nitrogen monoxide (O_3 -NO reaction), and the secondary reaction between ozone and nitrogen dioxide (O_3 -NO₂ reaction). This means that the reaction (k_1) occurs firstly when nitrogen monoxide is injected into the chamber. Nitrogen monoxide reacts with ozone to become nitrogen dioxide instantly because reaction (k_1) is a very rapid reaction, and then nitrogen dioxide is reduced by reactions (k_3) and (k_5). On the other hand, it is thought that dinitrogen pentoxide is increased by reaction (k_5) and converges to the concentration where the rates of reaction (k_5) and (k_6) become equilibrium.

(2) The case of reactions between ozone and nitrogen dioxide (O_3 -NO₂ reaction)

The concentration of ozone starts to reduce gradually after the injection of nitrogen dioxide, and the total amount of reduced ozone is nearly equal to that of the nitrogen dioxide injected (See Fig. 7).

The concentration of nitrogen dioxide is zero until it is injected, and then increases almost instantly by nearly the same amount as that of the injected nitrogen dioxide as seen in Fig. 9. After the initial increase, nitrogen dioxide is reduced more quickly than the case of reaction between ozone and nitrogen monoxide.

The absorptance of dinitrogen pentoxide varies as with the case of the reaction between ozone and nitrogen monoxide, but the constant on which the absorptance converged is a little smaller than that of the case of the reaction between ozone and nitrogen monoxide (See Fig. 11).

In this case, it is thought that the concentration of ozone is reduced mainly by reaction (k_3) which is a relatively slow reaction, therefore the concentration of ozone decreases gradually. The rate of the reduction of nitrogen dioxide is faster than that of the secondary O_3 -NO₂ reaction in the NO injection case, although chemical reactions in both cases are identical. This is most likely because the concentration of ozone in the NO₂ injection case is higher than that of the NO injection case, and rate of the reaction (k_3) is also higher.

3 Numerical Simulations of Ozone Change due to Chemical Reactions in Stratosphere

3.1 Governing Equation and Numerical Schemes

The governing equation for mass conservation of each species is written as [6]

$$\frac{\partial f_i}{\partial t} + \text{div}F_i = P_i - L_i f_i + E_i \quad (4)$$

where f_i , F_i , P_i , $L_i f_i$, and E_i are mass of species i , mass flux of species i , species mass generation rate by chemical reaction, species mass extinction rate, and species mass additional rate by artificial source, respectively.

In the two-dimensional analysis in coordinates system of latitude ϕ and altitude z , Eq.(4) can be reduced as

$$\begin{aligned} \frac{\partial f_i}{\partial t} + \frac{1}{a \cos \phi} \frac{\partial}{\partial \phi} (f_i v_i \cos \phi) + \frac{\partial}{\partial z} (f_i w_i) \\ = P_i - L_i f_i + E_i \\ + \frac{1}{a^2 \cos \phi} \frac{\partial}{\partial \phi} \left[K_{yy} \cos \phi \frac{\partial f_i}{\partial \phi} \right] + \frac{\partial}{\partial z} \left[K_{zz} \frac{\partial f_i}{\partial z} \right] \end{aligned} \quad (5)$$

where v_i and w_i are velocity components in latitude and altitude. K_{yy} and K_{zz} are turbulent diffusion coefficient in the corresponding directions. The diagonal terms of diffusion coefficient tensor K_{yz} and K_{zy} are neglected.

The numerical scheme of MPDATA (Multidimensional Positive Definite Advection Transport Algorithm) [7] is used for calculation of advection terms of Eq. (5). This scheme has an advantage of small numerical diffusion with up-wind finite difference by the recursive approach.

For the convection terms, the second-order central difference for space discretization and the Euler explicit method for time integration are used. A semi-implicit procedure is applied for the terms of chemical reaction in order to

**PREDICTION OF STRATOSPHERIC OZONE CHANGE DUE TO NITROGEN OXIDES
IN EXHAUST OF SUPERSONIC AIRPLANE**

avoid that the concentration of each species becomes negative.

3.2 Results and Discussion for Numerical Simulation

3.2.1 Computational conditions

The major conditions for numerical simulation are tabulated in Table 1 [4].

Table 1. Computational Conditions

Computational region	(a) 90 deg S – 90 deg N in latitude (b) 0 km - 50 km in altitude
Atmospheric temperature	Given as external input [8]
Atmospheric transport	Given as external input [8]
Chemical species	25 species including O ₃ and NO _x
Chemical reactions	82 reactions including 68 elementary reactions and 14 photo-dissociations [9]-[11]
Boundary conditions	(a) Solid wall at ground (b) Axisymmetric at north / south pole (c) First-order extrapolation at upper end
Initial condition	Natural atmospheric Condition [8]
Solar radiation	(a) Change of solar azimuth angle due to latitude and season is considered (b) Constant solar radiation at same latitude and season is assumed

3.2.2 Ozone concentration in natural condition

Calculated ozone number density in atmosphere in January is shown in Fig.12, where the altitude is presented by log-pressure. The ozone concentration distribution is compared with the observation [11] which

shows that the numerical simulation gives the good prediction except the altitude for the ozone concentration peak.

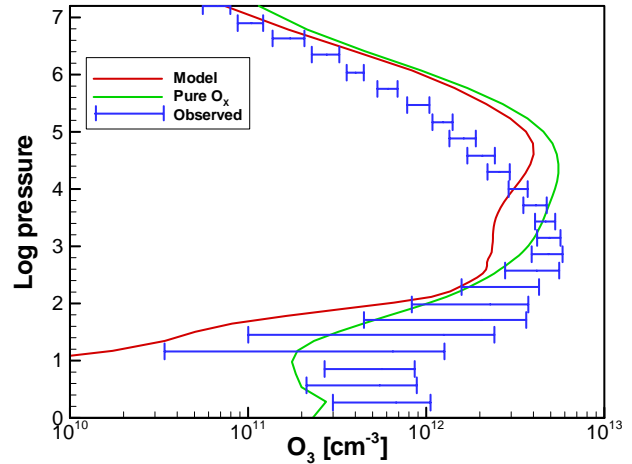


Fig. 12 Ozone Number Density in Natural Condition

3.2.3 Ozone change under the influence of flight of supersonic transport

The ozone concentration will be changed due to the chemical reactions with nitrogen oxides (NO_x) in the exhaust gas of supersonic transport. The ozone change was calculated along the NO_x exhaust scenario proposed by NASA [12] as tabulated in Table 2.

Table 2. NO_x Emission Scenario [12]

Exhausting altitude (km)	10, 20, 30
Exhausting latitude (degrees N)	40, 50, 60
Amount of exhausting NO _x (molecules/cm ³ /s)	500, 1000, 2000

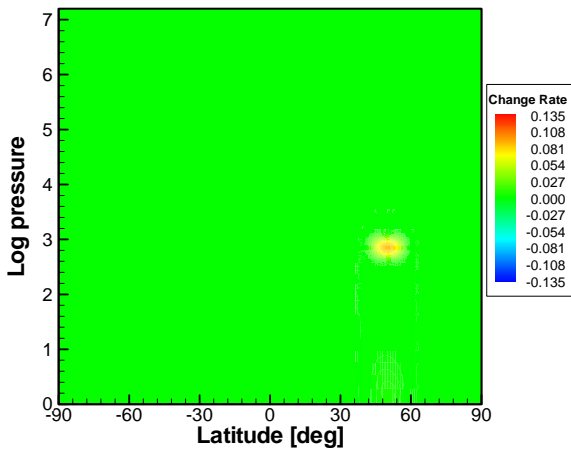
Amount of exhausting NO_x of 1000 molecules/cm³/s corresponds to an emission index (EI) of 10.6 for the fuel amount of 8.1 x 10¹⁰ kg.

An example of simulation results of ozone change is shown in Fig.13 for the case of amount of the emitted NO_x of 1000 molecules/cm³/s at exhausting altitude of 20 km, latitude of 50 degree N in April.

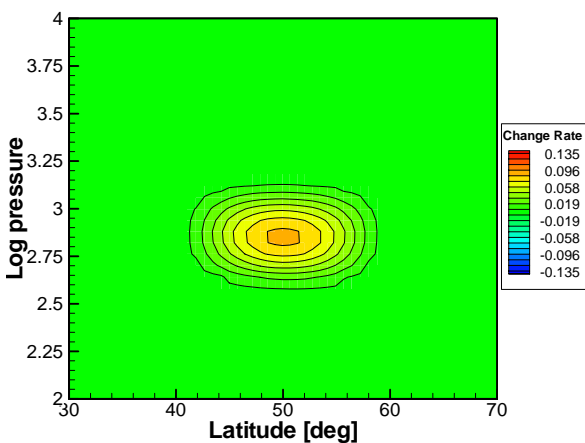
Figure 13 (a) and (b) illustrate the whole region of latitude between 90 degrees N to 90 degrees S and the close-up of the region

between 30 degrees N and 70 degrees N, respectively. There is no influence on ozone change in the southern hemisphere when the NOx is emitted in the northern hemisphere.

The log-pressure of 2.8 giving the maximum ozone change corresponds to the altitude of approximately 20 km. As shown in the ozone distribution pattern, ozone rather increases because that, in these altitude, O₃ generation due to the chemical reaction cycle related HOx (hydrogen oxides) is superior to O₃ depletion due to reaction with NOx [4].



(a) Latitude Range between 90 degrees S to 90 degrees N



(b) Latitude Range between 30 degrees N and 70 degrees N

Fig. 13 Ozone Change Rate for NOx Emission of 1000 Molecules/cm³/s at Altitude of 20 km and Latitude of 50 degrees N

The total ozone change rate calculated using the ozone concentration distribution for variation of amount of exhausting NOx is shown in Fig. 14 at exhausting altitude of 20 km, latitude of 50 degree N in January, where approximately 0.6 % – 1.9 % of total ozone generation is estimated for NOx emission of 500–2000 molecules/cm³/s. As easily expected, the more NOx emission is generated, the more ozone generation is estimated.

Figures 15 and 16 demonstrate the total ozone change rate for the cases of altitude of 10 km and 30 km at the same other conditions. The generation of ozone of approximately 4 % at NOx exhausting of 1000 molecules/cm³/s at 10 km can be seen, whereas ozone depletion of 0.4 % at 30 km is predicted.

As a result of these numerical simulations, generation of ozone will be expected in a lower altitude due to photo-chemical effect, however ozone depletion occurs at altitude around 30 km and over due to combined O₃ - NOx chemical reactions. These simulations are almost similar with the results of the Scenario F by NASA [12] of the conditions of Mach number of 2.4, exhausting altitude of 20 km, exhausting latitude of 50 degrees N and emission index of 15.

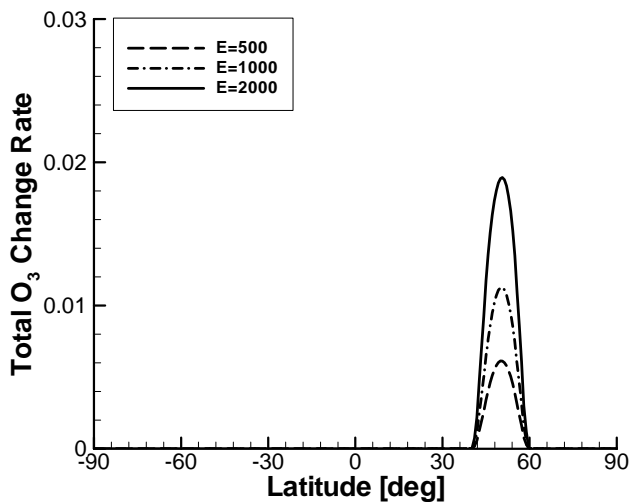


Fig. 14 Total Ozone Change Rate for NOx Emission of 500~2000 Molecules/cm³/s at Altitude of 20 km and Latitude of 50 degrees N

**PREDICTION OF STRATOSPHERIC OZONE CHANGE DUE TO NITROGEN OXIDES
IN EXHAUST OF SUPERSONIC AIRPLANE**

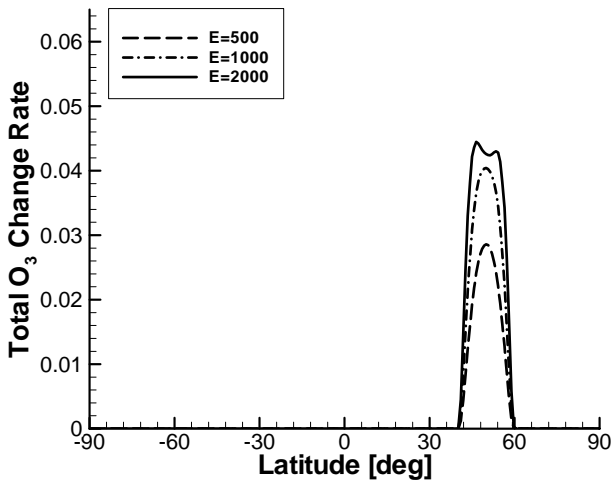


Fig. 15 Total Ozone Change Rate for NOx Emission of 500~2000 Molecules/cm³/s at Altitude of 10 km and Latitude of 50 degrees N

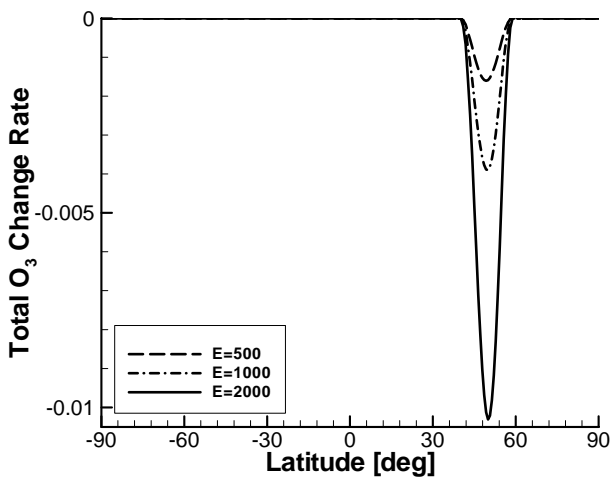


Fig. 16 Total Ozone Change Rate for NOx Emission of 500~2000 Molecules/cm³/s at Altitude of 30 km and Latitude of 50 degrees N

The effect of NOx exhaust in the range from latitude from 40 degrees N to 60 degrees N on ozone change seems very small.

4 Conclusions

Experiments of chemical reaction of ozone and nitrogen oxides in a space chamber and numerical simulation of ozone chemistry in the upper atmosphere with the flight scenario of

the supersonic transport were executed. The major conclusions are as follow:

- (1) As for space chamber experiments:
 - (a) The measurement technique for species concentration including ozone and nitrogen oxides using Fourier Transform Infrared Spectrometer (FT-IR) is established.
 - (b) The chemical reactions of ozone and nitrogen oxides are investigated by obtaining the adequate existing time history of each species in the simulated stratospheric condition.
 - (c) The nitrogen monoxide (NO) reacts quickly and nitrogen dioxide (NO₂) does slowly with ozone (O₃) in the O₃ – NOx reactions. Almost all species finally change into N₂O₅. It is verified that the considered chemical reactions and the associated reaction rates are appropriate through the comparison with analysis.
- (2) As for the numerical simulation:
 - (a) By using the numerical simulation, the natural ozone number density distributions are obtained and the effect of NOx exhaust on the ozone distribution is expected.
 - (b) Total ozone rather increases by NOx exhaust at the altitude below 20 km, but the possibility of ozone depletion is not denied when NOx is emitted around the altitude of 30 km and over.
 - (c) The effect of NOx exhaust on ozone layer is small in the latitude from 40 degrees N to 60 degrees N.

References

- [1] Japan Aircraft Development Corporation (JADC): URL; <http://www.jadc.or.jp/>, 2004.
- [2] Kubota H.: Technological and environmental issues for accomplishment of supersonic transport, Keynote Speech 1, *Proc. of JSASS (Japan Society for Aeronautical and Space Science) 16th International Sessions in 40th Aircraft Symposium*, pp. 5-8, 2002.
- [3] Ushiyama T, Watanuki T and Kubota H. Experimental simulation of ozone / NOx chemical

- reaction in consideration of experimental issues for next-generation supersonic transport. *Proc. of 4th Asian-Pacific Conference on Aerospace Technology and Science (4th ISCOPS)*, 2002.
- [4] Ushiyama T. A Study on effect of exhaust from supersonic transport on ozone layer. *Master thesis, Graduate School of Engineering, The University of Tokyo*, 2003.
- [5] Hiraishi J. (ed.), *Fourier Transform Infrared Spectroscopy*. Academy Press Center.
- [6] Jackman C H, Seals Jr R K and Prather M J. (ed) Two-dimensional intercomparison of stratospheric models. NASA CP 3042, 1989.
- [7] Smolarkiewicz P K. A fully multidimensional positive definite advection transport algorithm with small implicit diffusion. *Journal of Computational Physics*, Vol. 54, pp. 325-362, 1984.
- [8] University Corporation for Atmospheric Research (UCAR). URL; <http://www.ucar.edu/ucar/index.html>
- [9] World Meteorological Organization. Atmospheric ozone 1985. *Global Ozone Research and Monitoring Project*, Report 16, Vol.1-3 , 1985.
- [10] Kondratyev K Y. *Atmospheric Ozone variability, implications for climate change, human health and ecosystem*. Springer, 2000.
- [11] Matsuno T and Shimazaki T. *Atmospheric Chemistry Course 3, Atmosphere of Stratosphere and Mesosphere*. University of Tokyo Press, 1981.
- [12] International Aircraft Development Fund. *Study of Environmental Effect of the Next-Generation Supersonic Transport*, 2002.